Asian Journal of Chemistry; Vol. 37, No. 5 (2025), 1204-1210

ASIAN JOURNAL OF CHEMISTRY

https://doi.org/10.14233/ajchem.2025.33684

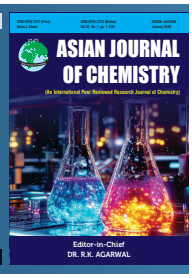

Spectroscopic and Optical Studies of Molybdenum Ions in CdO-SrO-B_2O_3-SiO_2 (CdSBSi) Glass System

J. Santhan Kumar[1,*], N. Rajya Lakshmi[1,2], K. Neeraja[3], T. Anjana Devi[4], D. Tirupathi Swamy[5], Shaik Azad Basha[1] and Sandhya Cole[1]

[1]Department of Physics, Acharya Nagarjuna University, Nagarjuna Nagar, Guntur-522510, India
[2]Department of General Section, Government Polytechnic College, Repalle-522265, India
[3]Department of Physics, Narasaraopet Engineering College, Narasaraopeta-522601, India
[4]Department of General Section, D.S.R. Government Polytechnic College, Ponnuru-522124, India
[5]Department of General Section, Government Polytechnic for Women, Guntur-522006, India

*Corresponding author: E-mail: santhanj007@gmail.com

Received: 15 March 2025; *Accepted*: 18 April 2025; *Published online*: 30 April 2025; AJC-21989

In this work, the electron paramagnetic resonance (EPR) and optical absorption investigations at room temperature have been conducted on MoO_3-CdO-SrO-B_2O_3-SiO_2 glasses by altering percentages of SrO and MoO_3. The distinctive EPR spectra of Mo^{5+} appeared at centered around g ~ 2.00 and are attributed to the Mo^{5+} ion within an axially distorted octahedral coordination sphere. Red shift was observed near an absorption edge in the UV spectra. The fundamental UV edges of absorption of the glasses were used to evaluate the Urbach energies and optical band gaps for transitions which occur directly or indirectly. A theoretical evaluation of glasses' optical basicity (Λ_{th}) has been conducted. The interaction between oxygen ligands and Mo^{5+} ions has been demonstrated to be improved. The covalent-to-ionic ratios of the glass can be classified using optical basicity, since a higher optical basicity indicates a lower degree of covalence.

Keywords: EPR, Molybdenum ion, Optical absorption, FT-IR, Borosilicate glass, Powder XRD.

INTRODUCTION

Glasses are super-cooled, transparent and amorphous liquids. After cooling in a rigid environment, these inorganic fusion products have not yet solidified. Long-range order in the crystal structure's existence is the primary difference between glass and crystals [1]. A comprehensive understanding of the microscopic structure of glass is essential for optimizing its properties based on composition and various processing factors. The characteristics of structural uniformity in glass represent a significant area of interest within the wider study of glass composition [2]. The applications of borosilicate glasses are extensive, encompassing a wide range of uses such as fiber composites, pharmaceuticals, sealing glasses, chemically resistant pipes and containers as well as the immobilization of nuclear wastes [3]. Rare earth oxide-doped borosilicate glasses have intriguing physical characteristics that make them suitable for use as laser host matrices [4].

The ceramic industry has long employed the strontium borosilicate system to create glass glaze coatings that are meant to be applied on porcelain, majolica, faience and other ceramic materials. High levels of the X-ray absorption coefficient, volume resistivity and refraction index are the characteristics of glass containing strontium [5,6]. Glass forming and liquid immiscibility areas in the SrO–B_2O_3–SiO_2 system have been investigated [7,8]. Data are presented on several physical parameters, including as density, micro-hardness, thermal expansion and viscosity.

The optical absorption and electron paramagnetic resonance (EPR) are the two important and practical methods for comprehending the microscopic characteristics of glasses. There has been a lot of interest in transition metal ion-containing glasses due to its prospective applications as magnetic materials [9], among others. Furthermore, they could be applied to the development of fiber-optic communication devices, tunable solid-state lasers and novel solar energy converters [10]. One

well-known glass former is MoO_3, in which molybdenum is present as Mo^{5+} ($^4d_1$ electron) [11]. Depending on their concentration, the Mo^{5+} cations may function as a network modulator or a network former. The glasses containing MoO_3 function as n-type semiconductors due to the minor polaron transition occurring from a Mo^{5+} to a Mo^{6+} site [12]. A deformed octahedral site has been proposed as the potential site symmetry in the ions of transition metals [13,14]. This study presents the optical absorption and EPR measurements of molybdenum ions in CdO-SrO-B_2O_3-SiO_2 (CdSBSi) glasses and also examines the influence of molybdenum on the density, molar volume and optical basicity.

EXPERIMENTAL

Glass preparation: To prepare a molybdenum doped CdSBSi glasses series, 99.9% pure starting components such as CdO, SrO, B_2O_3, SiO_2 and MoO_3 are utilized. Table-1 lists the components of each glass system sample. The optimum amounts of powdered materials were weighed using a digital scale with a ± 0.0001 g sensitivity, mixed well after crushed to a fine powder. In an electrical furnace, the batches were melted *in silica* crucibles for 10 to 15 min at temperatures that vary from 1475 K to 1525 K, based on their composition. A polished brass plate was then used to pour the melts onto and then quickly squeezed with another brass plate which leads to the clarity of glasses.

TABLE-1
COMPOSITION OF THE CdSBSi GLASS SYSTEM DOPED WITH DIFFERENT mol % OF MoO_3

Glass sample	CdO (mol %)	SrO (mol %)	B_2O_3 (mol %)	SiO_2 (mol %)	MoO_3 (mol %)
M_0	10	20.0	50	20	–
M_1	10	19.5	50	20	0.5
M_2	10	19.0	50	20	1.0
M_3	10	18.5	50	20	1.5
M_4	10	18.0	50	20	2.0
M_5	10	17.5	50	20	2.5

Characterization: The XRD patterns of glass samples were analyzed using the Philips PW (1710) Diffractometer consisting of copper target. For the optical measurements, the polished glasses wetre utilized. An X-band field modulation of 100 KHz was used in a JEOL-JM FE3 EPR spectrometer to record the EPR spectra of each glass sample at the ambient temperature. The optical absorption spectra of each glass sample at room temperature were recorded using a JASCO V-670 spectrophotometer, which measures the wavelengths between 200 and 1400 nm. Glass samples with a thickness of 1 mm were utilized for the optical testing. A Perkin-Elmer 577 Infrared spectrometer was used to measure the infrared absorption spectra of the room-temperature powdered glass samples using KBr method in the 4000–400 cm^{-1} wavenumber range.

RESULTS AND DISCUSSION

Physical characteristics: One of the most important methods for identifying the density measurement is based on the alterations to the glass network's structure. The various physical properties of the glass were assessed using standard equations [15], based on the computed average molecular weight (M) and density (d) of MoO_3-doped CdSBSi glasses. When the composition of glasses is slightly altered, the density vary suddenly. On the other hand, due to the spatial structure of the oxygen network, the molar volume of glass can be utilized to characterize the network structure and the arrangement of the construction units. In this work, the glass samples had densities between 3.586 and 3.667 g/cm^3 [16,17] and thus, these findings demonstrate that the density is not directly influenced by the concentration of MoO_3. However, both the molecular weight and density rates affect the molar volume. Nonetheless, three zones can be distinguished within this molar volume fluctuation (Table-2). The reason for the increase in the molar volume as the MoO_3 content reaches 1.0 mol% is the increase in the amount of NBOs in the first area. The molar volume is decreasing at a slow rate in the second zone. The non-bridging oxygen's constancy number could be the reason of this. A plausible explanation is that a significant amount of MoO_3 enters its structure directly, without requiring additional non-bridging oxygen. The formation of various structural units causes the molar volume to increase sharply once more in the third area (Table-2). Glass samples have molar volumes ranging from 23.236 to 23.772 cm^3/mol [18-20].

XRD studies: The obtained undoped and doped glasses' XRD spectra are displayed in Fig. 1 and the amorphous framework of the glasses is indicated and confirmed by the lack of crystalline peaks.

Optical absorption: The spectra of optical absorption of room-temperature MoO_3 ion-doped CdSBSi glasses measured in 200-1200 nm range are shown in Fig. 2. The absorption peak in pure glass occurs at 248 nm, but in glass M1, it is appears at 338 nm. When the amount of MoO_3 increases, a red shift was observed. Moreover, the spectra also show an apparent absorption band in the 600-800 nm range [21]. This shift can be explained by the significant absorption of Mo^{5+} in this spectral region. With

TABLE-2
PHYSICAL CHARACTERISTICS OF MoO_3 DOPED CDSBSI GLASSES

Glass sample	Mass (g)	Density (g/cm^3) (± 0.004)	Volume (cm^3)	Average molecular weight (M)	Transition metal ion conc. N_i (10^{20} ions/cm^3) ± 0.005	Inter ionic distance, r_i (Å) ± 0.005	Polar on radius, r_p (Å) ± 0.005	Molar volume
M_0	0.232	3.601	0.0646	85.29	–	–	–	23.687
M_1	0.646	3.602	0.1792	85.27	1.272	19.883	8.011	23.672
M_2	0.359	3.586	0.1000	85.26	2.533	15.803	6.367	23.772
M_3	0.822	3.652	0.2249	85.24	3.871	13.720	5.528	23.337
M_4	0.774	3.667	0.2109	86.22	5.184	12.448	5.015	23.236
M_5	0.332	3.658	0.0908	86.20	6.465	11.564	4.659	23.290

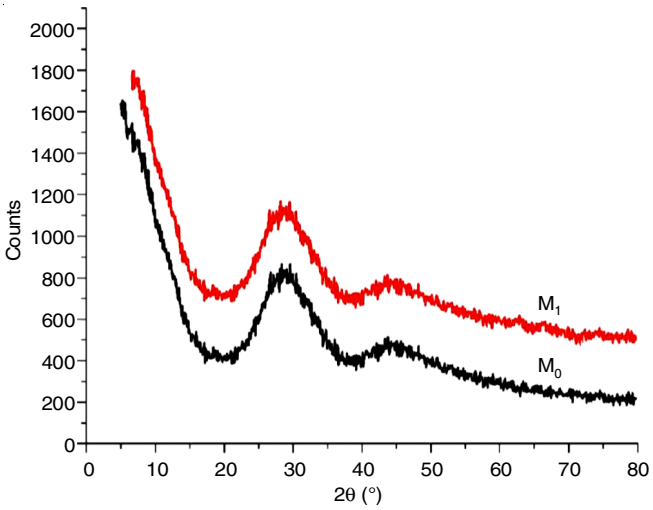

Fig. 1. X-ray diffraction patterns of undoped and MoO_3 doped CdSBSi glasses

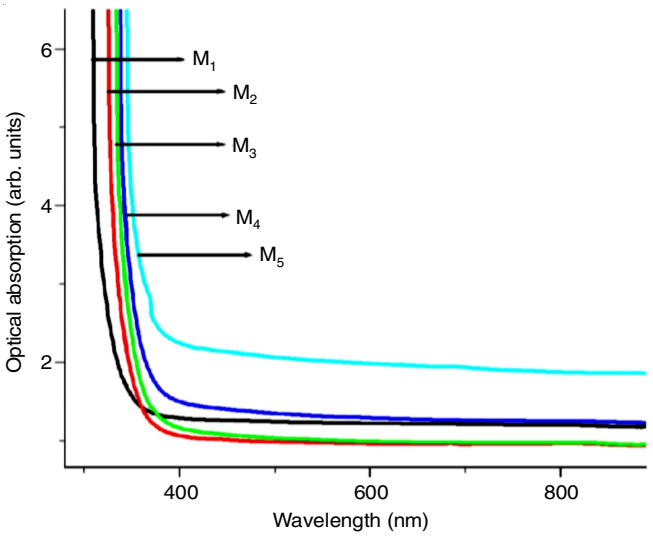

Fig. 2. Optical absorption spectra of MoO_3 doped CdSBSi glasses

a slight change in peak positions towards higher wavelengths, it was found that as the concentra-tion of MoO_3 increases, the half width of this band and its intensity grow non-linearly. Table-3 provides specifics on these optical absorption spectra of glasses.

TABLE-3
OPTICAL BAND POSITION VALUES OF MoO_3 DOPED CdSBSi GLASSES

Glass sample	Cut-off wavelength (nm)	Band position (nm) of Mo^{5+} ions
M_0	248	–
M_1	338	683
M_2	326	687
M_3	334	684
M_4	338	687
M_5	345	689

The excitation of the Mo^{5+} ($^4d_1$) ion causes the wide absorption band in the 600–800 nm range observed in the optical absorption spectra of these glasses. It has been anticipated that two optical excitations of this ion will occur, with E1 = 15,000 cm^{-1} and E2 = 23,000 cm^{-1}, originating from the b^2 (d_{xy}) ground state and moving on to ($d_{xz} - d_{yz}$) and ($d_{x^2-y^2}$). The inter-charge transfer of glass network ($Mo^{5+} \leftrightarrow Mo^{6+}$) may have prevented the resolution of these transitions. The glass spectra with the highest concentrations of MoO_3 and Mo^{5+} ions has the strongest intensity of this band. It is anticipated that these Mo^{5+} ions, which may exist as Mo^{5+} O^{3-} molecular orbital states, help in the depolymerization of glass network [22] by generating additional bonding defects due to the non-bridging oxygens (NBOs). Molybdenum ions penetrate interstitial spaces, nonetheless, the $Mo^{5+}O^{3-}$ complexes of oxygen generally disturb local symmetry [23-26].

Optical band gap: The Urbach energy and the optical band gap in CdSBSi glasses were measured with UV absorption spectroscopy. Both crystalline and non-crystalline semiconductors can undergo one of at their basic absorption edge, two kinds of optical transitions. There are both transitions, both direct and indirect. In mutual cases, the valence band electrons are elevated over the fundamental gap and interact with conduction band electromagnetic waves. Glass-forming anions have an impact on the conduction band in glasses, whereas cations play a minor but significant contribution [27-29]. Long-range order is encouraged and there are few flaws, as indicated by the sharp absorption edge or small ΔE.

The following formula can be used to find the α(ν) close to the peak:

$$\alpha(\nu) = \left(\frac{1}{d}\right)\ln\left(\frac{I_0}{I_t}\right) = 2.303\left(\frac{A}{d}\right) \quad (1)$$

The absorption coefficient α(ν) for both direct and indirect transitions as a function of photon energy (hν) was calculated using the following eqn. 2 [16]:

$$\alpha(\nu) = \frac{B(h\nu - E_{opt})^n}{h\nu} \quad (2)$$

where the index varies according to the mechanism of inter-bond transitions (n = 2 for direct transitions and n = 1/2 for indirect allowed transitions) and B is the energy-independent constant [17].

The hν plots can be extrapolated to get the values of the band gap energy, both direct and indirect E_{opt} in Fig. 3. Moreover, the graphs between ln (α) and hν were plotted (Fig. 4). In accordance with eqn. 3 [30], the reciprocal of the slopes in the linear section of curve in the lower photon energy region is utilized to determine the Urbach energy value (ΔE).

$$\alpha(\nu) = a_o \exp\left(\frac{h\nu}{\Delta E}\right) \quad (3)$$

Table-4 presents the optical band gaps for direct and indirect transitions, together with the determined Urbach energies.

EPR spectral studies: Fig. 5 displays the EPR spectra of CdSBSi glasses containing MoO_3. Less intense peaks encircle the central center line in the EPR spectra displayed in Fig. 5. Under the EPR inspection, the spectra of every pair of glasses showed a signal centered at g ~ 1.9 (Table-5). With natural abundances of 15.78% and 9.69% for odd ^{95}Mo and ^{97}Mo isotopes (I = 5/2), the peaks correlate to the hyperfine structure.

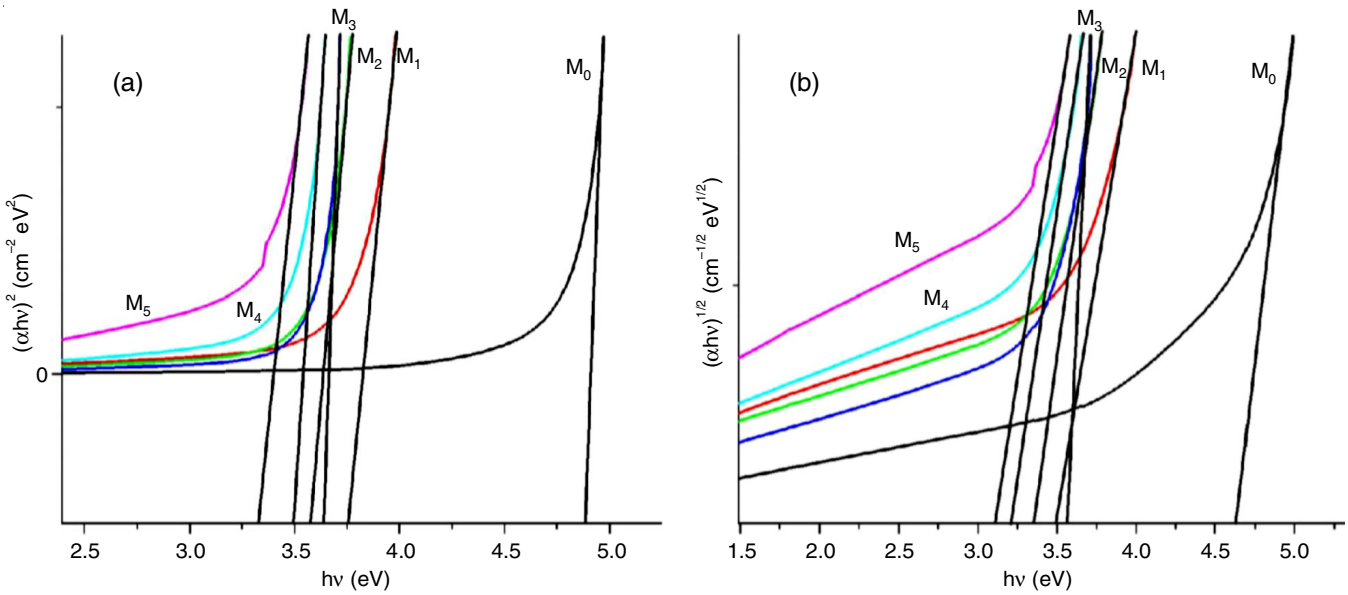

Fig. 3. (a) Direct bands and (b) indirect bands of MoO_3 doped CdSBSi glasses

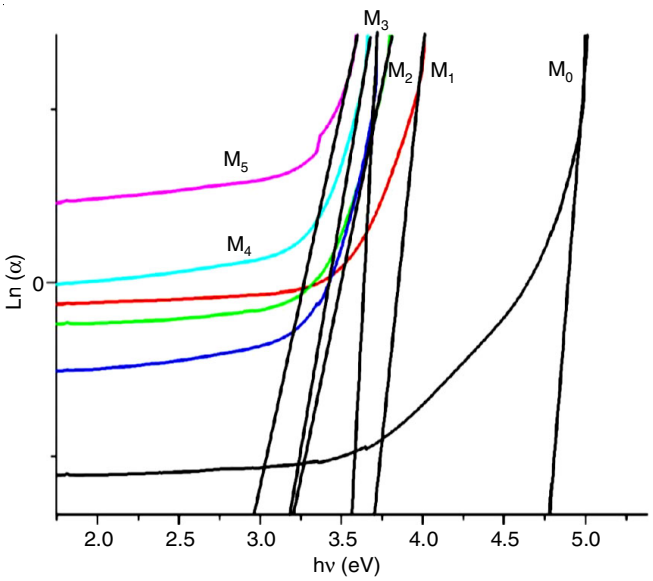

Fig. 4. Urbach plots of MoO_3 doped CdSBSi glasses

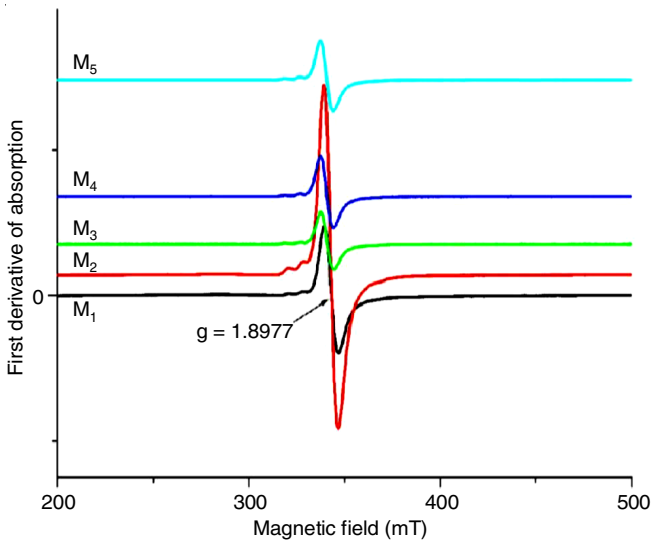

Fig. 5. EPR spectra of MoO_3 doped CdSBSi glasses

TABLE-4
DIRECT, INDIRECT AND URBACH ENERGY OF MoO_3 DOPED CdSBSi GLASSES

Glass sample	Direct (E_{opt}, eV)	Indirect (E_{opt}, eV)	Urbach (Δ_E, eV)
M_0	4.883	4.649	0.209
M_1	3.763	3.502	0.269
M_2	3.575	3.367	0.310
M_3	3.641	3.569	0.280
M_4	3.497	3.241	0.314
M_5	3.336	3.129	0.336

Moreover, they demonstrated that Mo^{5+} cation in the CdSBSi glasses has some axial distortion and an octahedral coordination of 18.25. An axially symmetric g-matrix is shown by the core I = 0 resonance signal's line shape. The form of the EPR spectra is shown to shift as the MoO_3 content of the samples increases.

TABLE-5
g AND OPTICAL BASICITY VALUES OF MoO_3 DOPED CdSBSi GLASSES

Glass sample	g value	Optical basicity
M_0	-	0.4356
M_1	1.8977	0.4352
M_2	1.9079	0.4348
M_3	1.8975	0.4344
M_4	1.9056	0.4341
M_5	1.9142	0.4337

The Mo^{5+} ions in the CdSBSi glasses under investigation likely show the minimal axial distortion and octahedral coordination. Since the core molybdenum's charge remains high, the oxygen ligands in the vicinity have a reduced effective charge and electron-donating capabilities, leading to an EPR shift. The two axial oxygens of the compressed octahedron thereby develop a strong π-bond. Furthermore, a significant displacement of Mo(V) inside its octahedral configuration A pyramidal MoO_5

configuration exhibiting an extremely short Mo–O distance, due to the molybdenyl ion, is used in this axially deformed setting [31-34].

Optical basicity (Λ_{th}): Based on the composition of the glass and the basicity moderating characteristics of the different cations present, the optimal values of optical basicity can be estimated. The ability of an oxide glass to supply a negative charge to a probe ion is determined by its optical basicity. Eqn. 2 was used to evaluate the theoretical values of the glass's optical basicity [35].

$$\Lambda_{th} = \sum_{i=1}^{n} \frac{Z_i}{2\gamma_i} \quad (6.1)$$

where n is the total number of cations present; Z_i is the oxidation number of the ith cation; γ_i is the ratio of the ith cations to the oxides present and i for the basicity regulating parameter of the ith cation. The basicity moderating parameter or i can be obtained using the formula below:

$$\gamma_i = 1.36\ (x_i - 0.26) \quad (6.2)$$

Pauling electrically negativity regarding the cation is represented by the symbol x_i. For every glass sample (Table-5), as seen in Fig. 6, the theoretical values of optical basicity (Λ_{th}) are computed as a function of Mo^{5+} content. Interestingly, as *x* increases, the optical basicity reduces linearly [36].

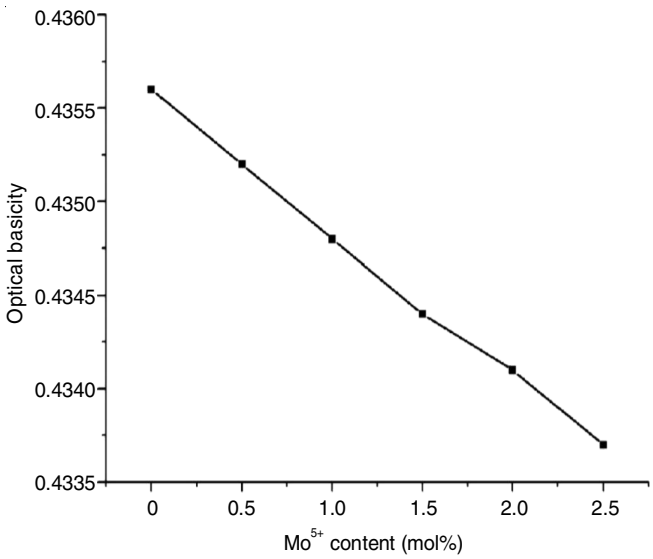

Fig. 6. Variation of theoretical values of optical basicity (Λ_{th}) of the CdSBSi glass samples as a function of Mo^{5+} content

FT-IR spectral studies: Investigations utilizing XRD analysis cannot determine the structural configuration of local glasses or the arrangement of their constituent units in relation to their nearest neighbours due to the absence of long-range order in glasses. IR vibrational spectra, on the other hand, can offer structural details and careful data analysis [37-39]. Furthermore, the existence of radiation-induced defects [40] or defect groups in a glass can be easily detected using vibrational spectra. Also, the low concentration contaminants like water, hydroxyl ions, *etc*. in glass have been identified using infrared spectroscopy [39].

Fig. 7 illustrates the FTIR spectra of MoO_3 doped CdSBSi glasses. Several frequency bands can be seen in the infrared spectra of the aforementioned glasses. The vibration bands at 4000-3450, 3450-2940 and 1700-1600 cm^{-1} show the stretching and deformation water can be either crystallized water, which is structurally connected with a component or coordination water in molecule form with OH groups. Therefore, the bands in the places are ascribed to the O-H-bond within the stretching glassy network. The Si-O-Si asymmetric vibration appears at 466 cm^{-1}, while the [BO_3] triangles' B-O-B bending vibration produces the minor shoulder at 698 cm^{-1}. The band intensity at 698 cm^{-1}, on the other hand, shows the same pattern of decreasing until $x = 1.0$ mol% and then increasing. The tetrahedral structural units of Si–O–Si and B–O–B network combined stretching vibrations produce the strong intensity band, which is between 1100 and 850 cm^{-1} [15,21,41]. This implies that although the weakest bands at 588, 524, 480, 426 and 405 cm^{-1}, the borate network is more prominent than the glass network. In this instance, the bands at roughly 698 cm^{-1} are produced by oxygen bonding between two trigonal boron atoms and one atom is trigonal, while one is tetrahedral.

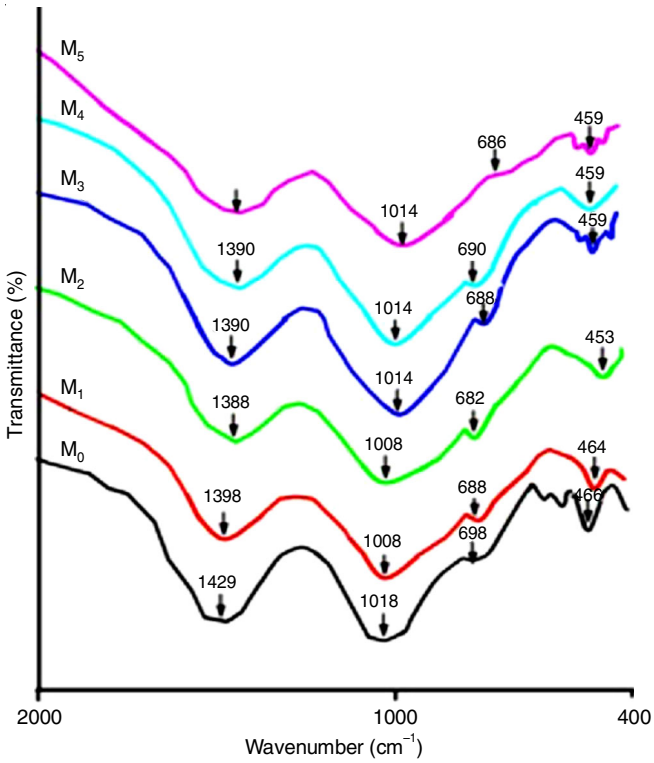

Fig. 7. FT-IR spectra of MoO_3 doped CdSBSi glasses

For glass M_2, the strength of this band decreases first, then increases and remains constant for the remaining samples. The wide shift, whose intensity ranges from 1018 cm^{-1}, distinguishes glass samples and shows that Mo^{5+} occurs in combination with octahedra. The prominent band of absorption at 1429 cm^{-1} is caused by the distinctive [BO_3] triangles' B-O stretching vibrations. Despite being present, SrO had no discernible effect. Table-6 compiles the data regarding the positions of the several band heads in the MoO_3 doped CdSBSi glasses [42-44].

TABLE-6
FT-IR SPECTRUM OF MoO_3 DOPED CdSBSi GLASSES

M_0	M_1	M_2	M_3	M_4	M_5	Assignment
1429	1398	1388	1390	1390	1392	Stretching vibrations of [BO_3]
1018	1008	1008	1014	1014	1014	Combined stretching vibrations of Si-O-Si and B-O-B
698	688	682	688	690	686	Bending vibration of B-O-B in [BO_3] triangles
466	464	453	459	459	459	Asymmetric vibration of Si-O-Si

Glasses M_3 and M_5 exhibit the bands at 430–400 cm^{-1} region, whereas, only glasses M_0 and M_5 exhibit the band at 590–550 cm^{-1}. Furthermore, the peak at 528-513 cm^{-1} is only visible in the glasses M_0 and M_5. As the amount of MOo_3 increases, the locations and intensities of the absorption bands in the glass network alter slightly. This implies that the molybdenum ion alters the network by presenting it as Mo^{5+} ion. The incorporation of SrO and CdO as network modifiers occurs between molybdenum ions and long-chain molecules, necessitating a modification of the glass's symmetry and covalency at the molybdenum ions [45].

Conclusion

In this work, MoO_3 doped CdO-SrO-B_2O_3-SiO_2 glasses were prepared by altering percentages of SrO and MoO_3 in a pure non-crystalline phase. The physical characteristics such as density values show that the concentration of MoO_3 is not a clear determinant and due to an increase in the non-bridging oxygen, the molar volumes increase as the concentration of MoO_3 does. All the prepared CdSBSi glasses exhibits red shift around the boundaries of the ultraviolet spectrum which is happened due to the significant Mo^{5+} absorption. The Urbach energy (ΔE) increases where the optical band gap's energy is (E_{opt}) falls as the molybdenum ion concentration increases. It has been found that both the optical band gap energy E_{opt} and the Urbach energy (ΔE) are impacted by the alkali ion's size. A sizable center line at g ~ 1.9 is visible in the EPR spectra of molybdenum ions in CdSBSi glasses, surrounded by lower intensity of satellite lines which is happened due to the slight axial distortion and octahedral coordination of the CdSBSi glasses containing Mo^{5+} cation. Furthermore, the Mo^{5+} ion, acting as a network modulator, is evident in the FT-IR spectra of the CdSBSi glasses.

ACKNOWLEDGEMENTS

One of the authors, Dr. Sandhya Cole, is grateful to The University Grants Commission, Government of India, New Delhi, India for granting the support under UGC-DRS program [File no. UGC-MRP F. No. 39-498/2010(SR)].

CONFLICT OF INTEREST

The authors declare that there is no conflict of interests regarding the publication of this article.

REFERENCES

1. Q. Zeng, H. Sheng, Y. Ding, L. Wang, W.Yang, J.-Z. Jiang, W.L. Mao and H.-K. Mao, *Science*, **332**, 1404 (2011); https://doi.org/10.1126/science.120032
2. X. Lu, J.D. Vienna and J. Du, *J. Am. Ceram. Soc.*, **107**, 1603 (2024); https://doi.org/10.1111/jace.19333
3. B. Karasu, I. Demirel, S. Aydin, M. Dalkiran and B. Lik, *El-Cezerî J. Sci. Eng.*, **7**, 940 (2020); https://doi.org/10.31202/ecjse.672615
4. Y.B. Saddeek, K.A. Aly and S.A. Bashier, *Physica B*, **405**, 2407 (2010); https://doi.org/10.1016/j.physb.2010.02.055
5. S.A.M. Issa, H.O. Tekin, M.M. Hessien and Y.S. Rammah, *J. Aust. Ceram. Soc.*, **58**, 495 (2022); https://doi.org/10.1007/s41779-022-00706-5
6. D.A. McKeown, W.K. Kot and I.L. Pegg, *J. Non-Cryst. Solids*, **317**, 290 (2003); https://doi.org/10.1016/S0022-3093(02)01816-1
7. R. Baylor Jr. and J.J. Brown Jr., *J. Am. Ceram. Soc.*, **59**, 131 (1976); https://doi.org/10.1111/j.1151-2916.1976.tb09449.x
8. S.V. Stolyar, N.G. Tyurnina, Z.G. Tyurnina and L.A. Doronina, *Glass Phys. Chem.*, **34**, 509 (2008); https://doi.org/10.1134/S1087659608040214
9. S.V. Stolyar and N.G. Tyurnina, *Glass Phys. Chem.*, **35**, 149 (2009); https://doi.org/10.1134/S1087659609020047
10. N.G. Tyurnina, Z.G. Tyurnina and S.I. Sviridov, *Glass Phys. Chem.*, **35**, 153 (2009); https://doi.org/10.1134/S1087659609020059
11. V.V. Golubkov, N.G. Tyurnina, Z.G. Tyurnina and V.L. Stolyarova, *Glass Phys. Chem.*, **35**, 455 (2009); https://doi.org/10.1134/S1087659609050010
12. Y. Liu, Y. Wang and J.S. Ma, *Key Eng. Mater.*, **336–338**, 783 (2007); https://doi.org/10.4028/www.scientific.net/KEM.336-338.783
13. C.-C. Chiang, S.-F. Wang, Y.-R. Wang and W.-C.J. Wei, *Ceram. Int.*, **34**, 599 (2008); https://doi.org/10.1016/j.ceramint.2006.12.008
14. H. Hirashima, Y. Watanabe and T. Yoshida, *J. Non-Cryst. Solids*, **95-96**, 825 (1987); https://doi.org/10.1016/S0022-3093(87)80687-7
15. M.M. Ahmed, C.A. Hogarth and M.N. Khan, *J. Mater. Sci.*, **19**, 4040 (1984); https://doi.org/10.1007/BF00980769
16. N.F. Mott and E.A. Davis, Electronic Processes in Non-Crystalline Materials, Oxford University Press: Oxford, edn, 2, p. 273 (1979).
17. J. Tauc, Amorphous and Liquid Semiconductor, Plenum: New York, (1974).
18. K. Subrahmanyam and M. Salagram, *Opt. Mater.*, **15**, 181 (2000); https://doi.org/10.1016/S0925-3467(00)00033-1
19. S. Simon and A.L. Nicula, *J. Non-Cryst. Solids*, **57**, 23 (1983); https://doi.org/10.1016/0022-3093(83)90405-2
20. A.M. Efimov, *J. Non-Cryst. Solids*, **203**, 1 (1996); https://doi.org/10.1016/0022-3093(96)00327-4
21. P.S. Prasad, B.V. Raghavaiah, R.B. Rao, C. Laxmikanth and N. Veeraiah, *Solid State Commun.*, **132**, 235 (2004); https://doi.org/10.1016/j.ssc.2004.07.042
22. L.S. Rao, M.S. Reddy, M.R. Reddy and N. Veeraiah, *J. Alloys Compd.*, **464**, 472 (2008); https://doi.org/10.1016/j.jallcom.2007.10.016
23. H. Darwish and M.M. Gomaa, *J. Mater. Sci. Mater. Electron.*, **17**, 35 (2006); https://doi.org/10.1007/s10854-005-5139-2
24. Y. Cheng, H. Xiao, W. Guo and W. Guo, *Ceram. Int.*, **33**, 1341 (2007); https://doi.org/10.1016/j.ceramint.2006.04.025
25. A.K. Hassan, L. Borjesson and L.M. Torell, *J. Non-Cryst. Solids*, **172/174**, 154 (1994); https://doi.org/10.1016/0022-3093(94)90427-8
26. E.I. Kamitsos, A.P. Patsis, M.A. Karakassides and G.D. Chryssikos, *J. Non-Cryst. Solids*, **126**, 52 (1990); https://doi.org/10.1016/0022-3093(90)91023-K

27. D.L. Griscom, *Glass Sci.*, **4**, 151 (1990); https://doi.org/10.1016/B978-0-12-706707-0.50010-4
28. H. Rawson, Inorganic Glass Forming Systems, Academic Press: New York (1967).
29. B.B. Das and R. Ambika, *Chem. Phys. Lett.*, **370**, 670 (2003); https://doi.org/10.1016/S0009-2614(03)00077-0
30. J.S. Kumar, V. Madhuri, J.L. Kumari and S. Cole, *Appl. Magn. Reson.*, **44**, 479 (2013); https://doi.org/10.1007/s00723-012-0409-7
31. A. Fluegel, *J. Am. Ceram. Soc.*, **90**, 2622 (2007); https://doi.org/10.1111/j.1551-2916.2007.01751.x
32. Y. Linard, H. Nonnet and T. Advocat, *J. Non-Cryst. Solids*, **354**, 4917 (2008); https://doi.org/10.1016/j.jnoncrysol.2008.07.013
33. S. Sindhu, S. Sanghi, A. Agarwal, V.P. Seth and N. Kishore, *Mater. Chem. Phys.*, **90**, 83 (2005); https://doi.org/10.1016/j.matchemphys.2004.10.013
34. A. Goldstein, V. Chiriac and D. Becherescu, *J. Non-Cryst. Solids*, **92**, 271 (1987); https://doi.org/10.1016/S0022-3093(87)80044-3
35. L. Bih, A. Nadiri, M. El Omari, A. Yacoubi and M. Haddad, *Phys. Chem. Glasses*, **43**, 153 (2002).
36. L. Bih, L. Abbas, A. Nadiri, H. Khemakhem and B. Elouadi, *J. Mol. Struct.*, **872**, 1 (2008); https://doi.org/10.1016/j.molstruc.2007.02.005
37. E.G. De Sousa, S.K. Mendiratta and J.M.M. Da Silva, *Portugal Phys.*, **17**, 203 (1986).
38. L. Pauling, The Nature of Chemical Bond, Cornell University Press, New York, edn. 3, p. 63 (1960).
39. J. Wong and C.A. Angell, Glass Structure by Spectroscopy, Marcel Dekker: New York (1976).
40. F.A. Khalifa, H.A. El-Batal and M.A. Azooz, *Indian J. Pure Appl. Phys.*, **36**, 314 (1998).
41. J.S. Kumar, J.L. Kumari, M.S. Rao and S. Cole, *Opt. Mater.*, **35**, 1320 (2013); https://doi.org/10.1016/j.optmat.2013.01.012
42. G. Fuxi, Optical and Spectroscopic Properties of Glasses, Springer, Berlin, p. 62 (1992).
43. P. Nachimuthu, P. Harikrishnan and R. Jagannathan, *Phys. Chem. Glasses*, **38**, 59 (1996).
44. E.A. Davis and N.F. Mott, *Philos. Mag.*, **22**, 903 (1970); https://doi.org/10.1080/14786437008221061
45. K. Nakamoto, Infrared Spectra of Inorganic and Coordination Compounds, edn 2, Wiley: New York, p. 98 (1963).